Protein Adsorption on Functionalized Multiwalled Carbon Nanotubes with Amino-Cyclodextrin

Lili Li, Wei Feng, and Peijun Ji

Dept. of Biochemical Engineering, Beijing University of Chemical Technology, Beijing 100029, China

Dept. of Chemical Engineering, Beijing University of Chemical Technology, Beijing 100029, China

DOI 10.1002/aic.12543

Published online February 28, 2011 in Wiley Online Library (wileyonlinelibrary.com).

A novel amino-cyclodextrin was synthesized, and it was covalently attached to multiwalled carbon nanotubes (MWNTs). The functionalized MWNTs (f-MWNTs) have very good aqueous dispersibility. Bovine serum albumin (BSA) was adsorbed onto f-MWNTs through noncovalent interactions, including the hydrophobic interaction of the residues of BSA with the wall of MWNT and the guest–host interaction of the residues with the cyclodextrin (CD) moieties of f-MWNTs. The ultraviolet–visible (UV–vis) absorption of the f-MWNT-BSA hybrid was measured with UV–vis spectrometer, and the absorbance can be described well with the Beer–Lambert law. The X-ray diffraction patterns have indicated that the crystalline form of BSA has been changed after the adsorption of BSA on f-MWNTs. The circular dichroism spectra have shown that a high percentage of α-helical content can be retained for BSA adsorbed on f-MWNTs. The results also indicate that the change of secondary structure of BSA is mainly due to the hydrophobic interaction of the residues of BSA with the wall of f-MWNT, whereas the secondary structure is much less affected by the interaction of the CD moieties with BSA. © 2011 American Institute of Chemical Engineers *AIChE J,* 57: 3507–3513, 2011

Keywords: amino-cyclodextrin, multiwalled carbon nanotubes, bovine serum albumin, secondary structure

Introduction

Carbon nanotubes (CNTs) have been paid great attention because of their extraordinary mechanical, electrical, and thermal properties as well as biocompatible property.[1–5] The sidewall surface of a pristine CNTs is highly hydrophobic, and bundles are formed mainly because of van der Waals interactions between the sidewalls of the individual tubes.[6] Surface functionality of CNTs[7] and individually dispersed CNTs in biocompatible media are very important for biological applications.[8] Proteins and enzymes are able to adsorb onto carbon nanotubes.[7,9] Streptavidin could form a highly ordered helical structure[10,11] covering the surface of multiwalled carbon nanotubes (MWNTs). β-Glucosidase, chymotrypsin, and soybean peroxidase were adsorbed at large quantities.[12,13] Bovine serum albumin (BSA) was adsorbed well and has been reported as an effective agent in dispersing CNTs.[12,13] Such functionalized CNTs can have good aqueous dispersibility. However, upon coating onto CNTs, the proteins had structural change.[14–17] The circular dichroism and Fourier transform infrared (FTIR) spectra reveal that the proteins undergo structural changes upon adsorption, and some proteins have significant loss of α-helical content.[14–17] As a result, the enzyme activity has been lost, for example,

Correspondence concerning this article should be addressed to W. Feng at fengwei@mail.buct.edu.cn; P. Ji at jipj@mail.buct.edu.cn.

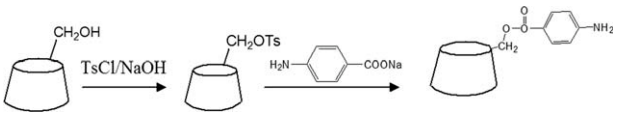

Figure 1. Synthesis of AmoBeno-β-CD.

soybean peroxidase retains up to 30% of its native activity upon adsorption, the adsorbed R-chymotrypsin retains 1% of its native activity,[14] and the enzymes[17] remain catalytically active upon adsorption onto CNTs with specific activities ranging from 40 to 70% relative to that of the native proteins. These results suggest that the proteins in the hybrids are partially unfolded. On the other hand, the protein adsorption on CNTs is generally carried out under sonication because of the formation of carbon nanotube bundles.[18] Sonication can create large pressure gradients,[19] while structural modifications of protein, such as loss of secondary structure, may be induced by the large pressure gradients.[20] During sonication, heat from the tip of the apparatus raises the temperature of the dispersion to $\sim$60–70°C,[18] whereas the secondary structure and conformation of proteins are cooperatively denatured on heating.[21] Under sonication, water-soluble proteins become partially unfolded.[18] The non-native hydrophobic domain of proteins exposed to the solvent interacts with the wall of CNTs, and the surface of the hybrid is covered with the hydrophilic groups of the protein. The protein–CNT hybrid contains the non-native hydrophobic domains of the protein and CNTs.[18]

The aim of this study is to functionalize MWNTs and make MWNTs have good aqueous dispersibility and be compatible with proteins. A novel cyclodextrin derivative is synthesized, which is utilized to covalently attach onto MWNTs. BSA was adsorbed onto functionalized MWNTs (f-MWNTs) through noncovalent interaction. Ultraviolet–visible (UV–vis) absorption of f-MWNT-BSA was described by the Beer–Lambert law. The interaction of BSA with f-MWNTs was investigated through XRD patterns and circular dichroism spectra. The secondary structure change of BSA adsorbed on f-MWNTs was monitored by circular dichroism and FTIR spectra.

Experiment

Materials

Multiwalled carbon nanotubes (MWNTs) (purity >95%, diameter within 5–10 nm) were purchased from Nacen Nanotechnologies. Bovine serum albumin (BSA), *N*-ethyl-*N*-(3-(dimethylamino)propyl)carbodiimide hydrochloride (EDC), 2-(*N*-morpholino) ethanesulfonic acid (MES), *N*-hydroxysuccinimide (NHS), β-cyclodextrin, 4-aminobenzoic acid sodium salt (AmBenoNa), and *p*-toluenesulfonyl chloride (TsCl) were purchased from Sigma-Aldrich Chemical, China, and the chemicals were used without further purification. Deionized double-distilled water was used for making the solutions.

Purification and oxidation of MWNTs

MWNTs were purified and oxidized as reported by Liu et al.[22] As-received MWNTs were purified by refluxing in an aqueous HNO_3 of 2.6 M at 70°C for 45 h. The nanotube suspension was diluted and washed with double-distilled water by filtering through a 0.8-μm polycarbonate membrane. The samples were dried at 80°C under vacuum. The purified MWNTs (p-MWNTs) were further oxidized in the 3:1 concentrated H_2SO4:HNO_3 mixture for 3 h. The nanotube suspension was diluted and washed with double-distilled water by filtering through a 0.45-μm polycarbonate membrane. The samples were dried at 80°C under vacuum.

Preparation of the cyclodextrin derivative of AmoBeno-β-CD

The cyclodextrin derivative mono-6-deoxy-6-(4-aminobenzoyl)-β-CD (AmoBeno-β-CD) (Figure 1) was prepared as follows. The 6-*O*-monotosyi-6-deoxy-β-cyclodextrin (6-TsO-CD) was synthesized by the reaction of *p*-toluenesulfonic anhydride with β-cyclodextrin as described in literatue.[23] 6-TsO-CD (3g) and AmBenoNa (1 g) dissolved in DMSO (60 ml) were incubated at 80°C for 3 days. After being cooled to room temperature, the solution was poured into acetone. The precipitate was washed by filtering through a 0.2-μm polycarbonate membrane and dried under vacuum at 60°C. Then, DIAION HP-20 column chromatogyaphy[24] was used to purify the precipitate. The fraction eluted with the eluent of water/methanol (80/20) was concentrated and dried under vacuum to get AmBeno-β-CD. The H NMR (DMSO-d_6, 600 MHz) confirmed the synthesis of 6-AmBeno-β-CD: δ 7.56 (d, 2H, 2H of phenyl), δ 6.43 (d, 2H, 3H of phenyl), 6.11 (m, 14H, O(2)H and O(3)H of CD), δ 5.13 (s, 2H, NH_2), 4.82 (m, 7H, C(1)H of CD), 4.44–4.35 (m, 6H, O(6)H), 3.66–3.56 (m, 21H, C(6)H and C(3)H), 3.45–3.29 (m, 14H, C(2)H and C(5)H).

Preparation of AmoBeno-β-CD-MWNT (f-MWNT)

Figure 2 shows the functionalization of MWNTs with AmoBeno-β-CD. Oxidized MWNTs (50 mg) and NHS (2.3 g) were added to 100-ml MES buffer (pH 6.2, 50 mM). A homogeneous suspension was obtained by bath sonicaton for 30 min. To this suspension, EDC·HCl (0.38 g) was added, and then the mixture was stirred at 150 rpm for 30 min. The activated nanotubes were rinsed thoroughly with MES buffer to remove excess EDC and NHS by filtering through a

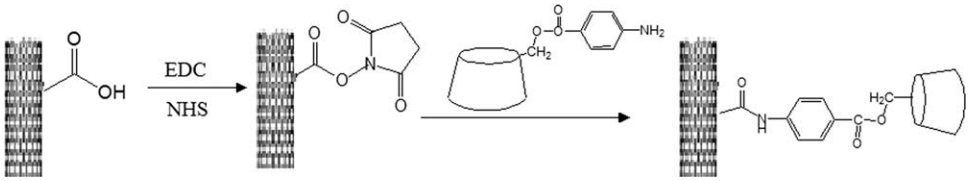

Figure 2. Functionalization of MWNTs with AmoBeno-β-CD.

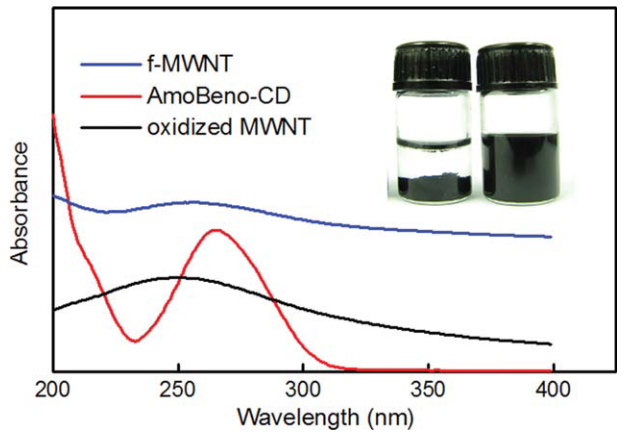

Figure 3. UV–vis spectra of f-MWNTs (blue), oxidized MWNTs (black), and AmoBeno-CD (red) in aqueous solution.

Insert: photos of aqueous solutions with oxidized MWNTs (left) and f-MWNTs (right). [Color figure can be viewed in the online issue, which is available at wileyonlinelibrary.com.]

polycarbonate membrane (0.2 μm). The nanotube film was transferred to the aqueous solution of AmoBeno-β-CD (2.8 g) and sonicated for 15 min to redisperse the nanotubes. The mixture was shaken (150 rpm) at room temperature for 4 h. The suspension of AmoBeno-β-CD-MWNTs (f-MWNTs) was washed by filtering through a polycarbonate membrane (0.2 μm) and dried under vacuum.

Determination of the saturation adsorption of protein onto f-MWNTs

BSA with different concentrations (0.0075–0.025 mg/ml) was added into the aqueous solution of f-MWNT (0.025 mg/ml), and the mixture was then shaken at 20°C in a incubator shaker at 150 rpm for 4 h. The nanotube-BSA suspension was then washed with double-distilled water by filtering through a polycarbonate membrane (0.2 μm). The amount of BSA in the filtrate was determined by UV–vis spectra, which were measured using a Shimadzu spectrophotometer (model UV 2550) operated at a resolution of 1 nm. The saturation adsorption of protein onto f-MWNTs was determined through the BSA detection in the filtrate.

Description of UV–vis absorption of f-MWNT-BSA based on the Beer–Lambert law

The Beer–Lambert law[25] was applied to describe the UV–vis absorption of f-MWNT-BSA. As the f-MWNTs have very good aqueous dispersibility, a spectrum of f-MWNTs alone at a known concentration can be obtained. A spectrum of the two constituents together in a known composition was obtained by mixing a known quantity of f-MWNTs with a known quantity of BSA. Thirty samples were prepared, and the concentration range was 0–1.5 mg/ml and 0–0.05 mg/ml for BSA and f-MWNTs, respectively. The spectra were measured in the 250- to 750-nm range with 2-nm intervals for analysis, using double-distilled water as the blank measurement.

Calculations of UV–vis absorbance were based on Beer–Lambert law: when the spectra of a mixture of two constituents overlap, the absorbance of the constituents at the same wavelength, λ, is additive, and the Beer–Lambert law takes the following form[23]

$$A_\lambda = \varepsilon_{\lambda,\mathrm{a}} \cdot l \cdot C_\mathrm{a} + \varepsilon_{\lambda,\mathrm{b}} \cdot l \cdot C_\mathrm{b} \tag{1}$$

where A is the absorbance, C is the concentration, ε is the extinction coefficient, and l is the length traveled by light through the specimen. As l is constant through the experiments, a k parameter is defined as: $k_{\lambda,i} = \varepsilon_{\lambda,i} \cdot l$. Then, Eq. 1 can be expressed as

$$A_\lambda = k_{\lambda,\mathrm{a}} C_\mathrm{a} + k_{\lambda,\mathrm{b}} C_\mathrm{b} \tag{2}$$

At each wavelength, λ, two parameters, $k_{\lambda,\mathrm{a}}$ and $k_{\lambda,\mathrm{b}}$, must be determined to calculate the absorbance A_λ. The two parameters are obtained by fitting to the experimental data of UV–vis absorbance. Following objective function is adopted for the regression

$$\mathrm{Func} = \sum_{i=1}^{30} \left| \frac{A_\lambda^i(\mathrm{cal}) - A_\lambda^i(\mathrm{exp})}{A_\lambda^i(\mathrm{exp})} \right| \tag{3}$$

For each wavelength, 30 data of absorbance were used for the regression to determine the two parameters. The program used for the regression is developed based on the regression subroutine (Levenberg–Marquadt nonlinear least squares).[26]

Secondary structure detected with circular dichroism spectroscopy

Circular dichroism spectroscopy was used to monitor the secondary structure of BSA adsorbed on f-MWNTs. The circular dichroism spectra (190–260 nm) were recorded on a JASCO J-810 CD instrument (JASCO) with a bandwidth of 0.5 nm and a scan speed of 50 nm/min, and the cell length was 10 mm. The main parameters of circular dichroism including band width, sensitivity, and scanning speed were set at 1 nm, 100 mdeg, and 1000 nm/min, respectively. The concentrations were 0.0075–0.05 mg/ml for BSA and 0.025 and 0.05 mg/ml for f-MWNTs, respectively. Circular dichroism spectra of the f-MWNTs were recorded similarly as a control. The circular dichroism spectrum of BSA adsorbed on f-MWNTs was corrected by subtracting the spectrum of f-MWNTs. Each scan was repeated five times, and the spectra were then averaged. CDPro software (http://lamar.colostate.edu) was used for analyzing the circular dichroism spectra of BSA.

FTIR spectrum

A Varian FTIR Spectrometer with an attenuated total reflectance attachment was used for the measurement of FTIR spectra.

XRD measurement

The XRD patterns were obtained with a powder diffractometer of Rigaku D/Max 2500 VBZ+/PC using a Gu target at 35 kV, 30 mA. The powder diffractograms were operated at a scan rate of $2\theta = 1°$/min from $2\theta = 5°$ to $2\theta = 90°$.

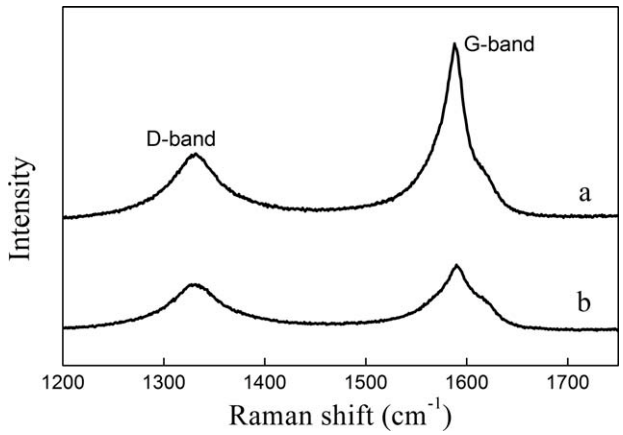

Figure 4. Raman spectra of f-MWNTs (a) and oxidized MWNTs (b).

Results and Discussion

Functionalization of MWNTs

MWNTs were functionalized by the reactions of carboxylic acid groups of oxidized MWNTs with AmoBeno-CD. Figure 3 presents the UV–vis absorption. As can be seen, the absorbance of AmoBeno-CD (red) and oxidized MWNTs (black) is reflected in the absorbance of f-MWNTs (blue). Compared to the absorbance peak of oxidized MWNTs at 252 nm, the absorbance peak of f-MWNTs is shifted to 258 nm. The functionalized MWNTs have a good aqueous dispersibility as shown in the insert of Figure 3, and the suspension was stable after 3 months. The functionalization was also confirmed by the Raman spectra as shown in Figure 4. Because of the covalent attachment of the amino-cyclodextrins, the peak intensity ratio of the main peak (G-band) to the broad peak (D-band) is increased from 1.35 of the oxidized MWNTs to 1.60 of f-MWNTs.[27,28]

Calculation of the UV–vis absorbance of f-MWNT-BSA

Figure 5 presents the results of the comparison between the calculation (dashed lines) and measurement (solid lines); the lines in blue are for f-MWNT-BSA, red for f-MWNT, and black for BSA. The absorbance data of the sample of f-MWNT-BSA were used to determine the two parameters required by the Beer–Lambert law. For f-MWNT-BSA, the recalculated line fits the data very well with a relative deviation of 0.67%, as presented by lines in blue. Using the obtained two parameters, the spectra of f-MWNTs and BSA were predicated. The calculated lines have a good agreement with the data, with relative deviations 2.33 and 1.17% for f-MWNTs and BSA, respectively. The result of Figure 5 indicates that the Beer–Lambert law can be applied to describe f-MWNT-protein hybrids. Through UV–vis measurement, the saturation adsorption of BSA onto f-MWNTs is about 0.6 mg of BSA/mg of f-MWNTs.

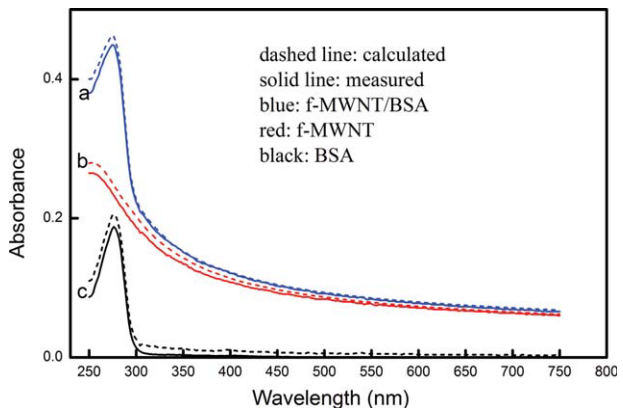

Figure 5. UV–vis absorbance.

f-MWNT-BSA (blue), f-MWNTs (red), and BSA (black). Concentrations: BSA 0.185 mg/ml and f-MWNTs 0.004 mg/ml. [Color figure can be viewed in the online issue, which is available at wileyonlinelibrary.com.]

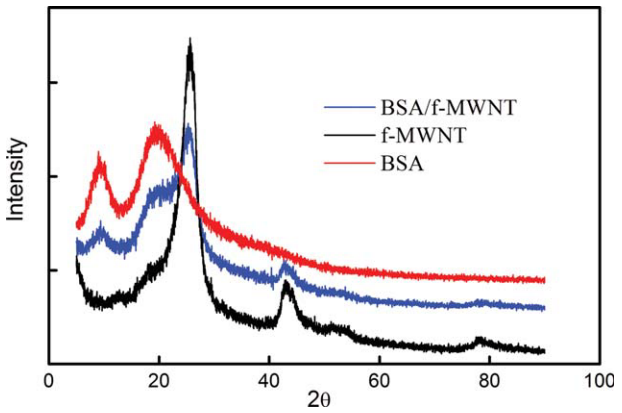

Figure 6. XRD patterns.

f-MWNT (black), BSA (red), and f-MWNT-BSA (blue). [Color figure can be viewed in the online issue, which is available at wileyonlinelibrary.com.]

X-ray diffraction

Figure 6 shows XRD patterns for BSA, f-MWNTs, and f-MWNT-BSA. The XRD pattern of the f-MWNT-BSA sample (in blue) presents a prominent peak at $2\theta = 25.6°$ and a smaller peak at $2\theta = 42.8°$, which are the typical peaks for carbon nanotubes. The XRD pattern also indicates that the CD moieties on f-MWNTs are not in crystalline form. BSA alone (in red) presents sharp peaks at $2\theta = 9.1°$and $2\theta = 19.5°$. In the XRD pattern of f-MWNT-BSA, the two peaks of BSA are shifted to $2\theta = 9.4°$ and $2\theta = 21.0°$, respectively. Compared to the sharp peak of native BSA at 19.5°, the peak for the BSA adsorbed on f-MWNT at $2\theta = 21.0°$ becomes broader. The results indicate that the interaction of BSA with f-MWNTs has changed the crystalline form of BSA. Some crystalline formation of the BSA adsorbed on f-MWNT may be due to the uneven distribution of the BSA on the wall of f-MWNT, as shown in Figure 7 of the high-resolution TEM.

Secondary structure analysis by circular dichroism

Carbon nanotubes have a natural affinity for diverse proteins mainly through hydrophobic interaction.[10] Ring structures in aromatic amino acids (e.g., phenylalanine and tryptophan) are important for the interaction between the protein and CNTs through π-stacking.[29] Cyclodextrins can be visualized as toroidal, hollow, truncated cones with hydrophilic rims, the internal cavity is hydrophobic.[6] The unique molecular structure makes cyclodextrins have the ability to sequester hydrophobic moieties on protein surfaces.[30] The

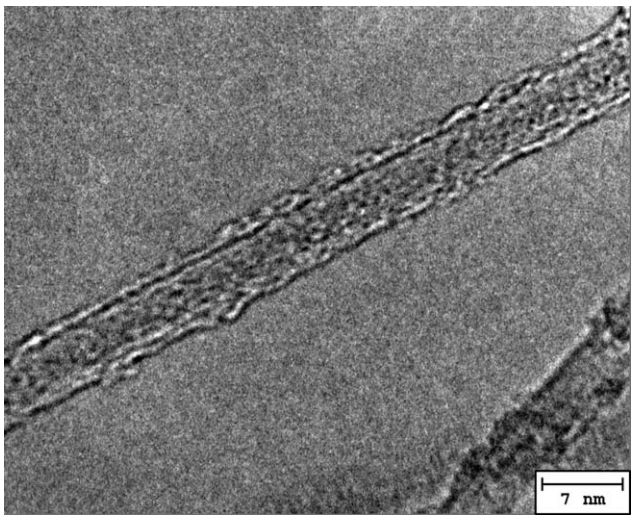

Figure 7. HRTEM image of f-MWNTs attached by BSA.

adsorption is spontaneous when BSA comes in contact with f-MWNTs in water and follows a pseudosaturation behavior.[9] The CD moieties are distributed at the defect sites of the wall and the tips of f-MWNTs. Upon the adsorption of BSA on f-MWNT, there are two types of interactions: the interaction of the aromatic amino acids of BSA with the walls of f-MWNTs, and the CD moieties have a guest–host interaction with BSA through forming weak inclusion complexes with aromatic residues.

Circular dichroism spectra were analyzed for the change of secondary structure of the BSA adsorbed on f-MWNTs. Figure 8a illustrates the circular dichroism spectra for the BSA adsorbed on the purified MWNTs (p-MWNTs) under sonication for 10 min (red) and under shaking (olive) for 2 h as well as for the BSA adsorbed on f-MWNT under shaking (blue) for 2 h. Compared to the line (black) for the native BSA, the α-helix retained, corresponding to the red, olive, and blue lines, are 69.8, 74.9, and 82.4%, respectively. These results show the advantage of f-MWNTs over p-MWNTs in preserving the secondary structure of BSA upon adsorption. This is due to two reasons: f-MWNTs have very good aqueous dispersibility, and the adsorption of BSA onto f-MWNTs is facilitated and can be carried out under shaking instead of sonication; on the other hand, the origin of the results has been suggested to be a specific interaction between CD moieties and hydrophobic amino acids of BSA. This interaction is favorable to prevent the unfolding of proteins.[31] To elucidate the function of CD moieties in preserving the protein structure, the spectrum of β-CD-BSA at the weight ratio of BSA to β-CD of 0.56 was measured. The ratio of β-CD to BSA (1/0.56) is much larger than the ratio of the CD moieties to BSA, as the CD moieties are only at the defect sites and tips of f-MWNTs. The measured spectrum is presented in Figure 8b, and the α-helix retained is about 92%. From the spectra in Figures 8a, b, it can be concluded that the change of secondary structure induced by the hydrophobic interaction between BSA and f-MWNTs is larger than that induced by the guest–host interaction between CD moieties and BSA. The role of the CD moiety in preserving the secondary structure of BSA is consistent with the work published.[32–34] The interaction of cyclodextrins with proteins has shown that[32–34] cyclodextrins have the ability to refold protiens from denatured states or to inhibit the aggregation of proteins.

In Figure 8c, the spectra were measured at different weight ratio of BSA to f-MWNTs at 25°C. It can be seen that the change of the secondary structure decreases with the increasing of the weight ratio of BSA to f-MWNTs. After the saturation adsorption, the presence of excess unadsorbed protein contributes to the enhancement of α-helix retained. The spectra before the saturation adsorption further confirm that the hydrophobic interaction between the residues and the wall of f-MWNT is the main reason leading to the partial unfolding of BSA upon adsorption. This conclusion can be supported by the published results of adsorption of proteins on carbon nanotubes, the proteins undergoing structural changes upon adsorption.[14,15] The losses in the α-helical content due to the adsorption onto CNTs for soybean peroxidase and R-chymotrypsin (CT) are 22 and 43%, respectively.[14]

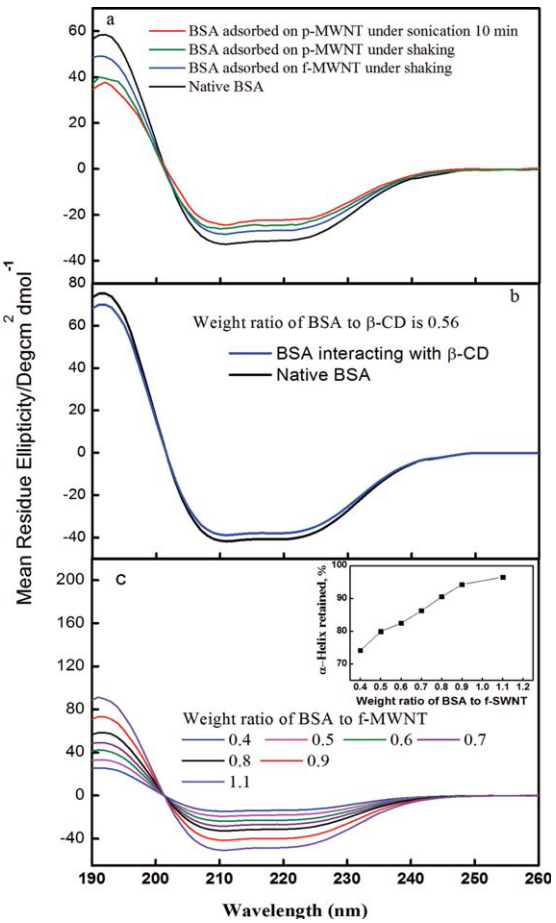

Figure 8. Circular dichroism spectra: (a) BSA adsorbed on p-MWNTs under sonication (red) and under shaking (olive); BSA adsorbed on f-MWNTs under shaking (blue); native BSA (black).

The weight ratio of BSA to CNTs is 0.6. (b) BSA interacting with β-cyclodextrins. Concentrations: β-cyclodextrins (0.036 mg/ml) and BSA (0.02 mg/ml). (c) At different weight ratios of BSA to f-MWNTs. Insert: percentage of α-helix retained. [Color figure can be viewed in the online issue, which is available at wileyonlinelibrary.com.]

Horseradish peroxidase endures a loss of about 35% in the α-helical content of its secondary structure.[15]

Secondary structure by Fourier transform infrared spectra

The amide I (1600–1700 cm^{-1}) region of the FTIR spectrum of a protein has been widely used to quantify the individual elements of the secondary structure.[35,36] In this study, the percentage of α-helix determined from the amide I spectral region was used to look at the structural perturbations of BSA when adsorbed on f-MWNTs. In the measurement of the FTIR spectrum of the BSA adsorbed on f-MWNTs, FTIR spectrum of f-MWNTs was recorded as a control. Figure 9 shows FTIR spectra of BSA and f-MWNT-BSA in the amide I region. Using the second-derivative method, Peakfit software was applied to analyze the secondary structural features. α-Helical and β-sheet structures were assigned following the reports in literature,[35] and their relative amounts were determined by computing the areas under the assigned bands. Gaussian deconvolution of the spectrum revealed an α-helical content of 34.7% for f-MWNT-BSA compared to an α-helical content of 50.1% for the native BSA, as listed in Table 1. The BSA adsorbed on f-MWNTs retains 81.3% ± 0.4% of the α-helical content of the native BSA. This result is comparable to the change of secondary structure monitored by the circular dichroism spectrum (blue) as presented in Figure 8a.

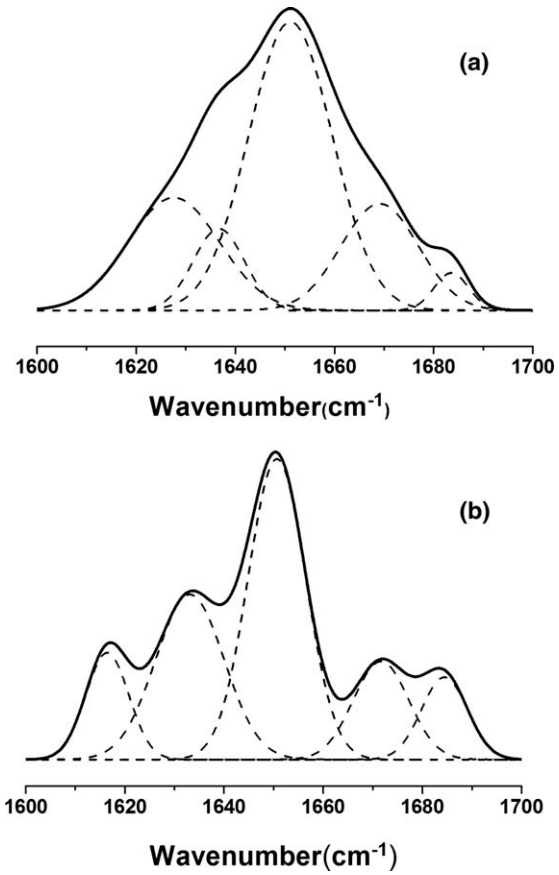

Figure 9. Fourier self-deconvoluted FTIR spectra and Gaussian curve fitting.

(a) Native BSA and (b) f-MWNT-BSA. The weight ratio of BSA to f-MWNTs is 0.6.

Table 1. Band Position and Assignments for the Native and Adsorbed BSA

Sample	Second-Derivative Band Position	Assignment	Area (%)
Native BSA	1627.6	Other	21.4
	1636.7	β-Sheet	8.68
	1651.1	α-Helix	50.1
	1669.1	β-Sheet	17.1
	1683.6	Other	2.72
Adsorbed BSA	1610.2	Other	1.79
	1623.3	Other	22.4
	1636.5	β-Sheet	13.6
	1650.7	α-Helix	34.7
	1669.7	β-Sheet	21.4
	1683.8	Other	6.11

Conclusions

MWNTs were functionalized with a novel amino-cyclodextrin synthesized. The protein BSA was adsorbed on f-MWNTs through noncovalent interactions. The Beer–Lambert law was able to describe the UV absorbance of the f-MWNT-BSA hybrid with good accuracy. The XRD patterns have shown that the BSA adsorbed on f-MWNTs has changed its crystalline form. The circular dichroism spectra have shown that a high percentage of α-helical content can be retained when BSA is adsorbed on f-MWNTs. The results also indicate that the change of secondary structure of BSA is mainly caused by the hydrophobic interaction of the residues of BSA with the walls of f-MWNTs, whereas the secondary structure is less affected by the interaction of the CD moieties with BSA. This work demonstrates that, with the amino-cyclodextrain to functionalize carbon nanotube, the f-MWNTs can have very good aqueous dispersibility; this facilitates the adsorption of BSA onto f-MWNTs. On the other hand, the CD moieties can contribute to the preservation of protein structure in the process of adsorption.

Acknowledgments

This work was supported by the National Science Foundation of China (21076018, 20636010), the National Basic Research Program of China (2007CB714302, 2011CB200905), the 863 Program (2009AA033001), and the Program for New Century Excellent Talents in University.

Literature Cited

1. Moulton SE, Minett AI, Murphy R, Ryan KP, McCarthy D, Coleman JN, Blau WJ, Wallace GG. Biomolecules as selective dispersants for carbon nanotubes. *Carbon*. 2005;43:1879–1884.
2. Zhang P, Henthorn DB. Synthesis of PEGylated single wall carbon nanotubes by a photoinitiated graft from polymerization. *AIChE J*. 2010;56:1610–1615.
3. Charlie Johnson AT, Staii C, Chen M, Khamis S, Johnson R, Klein ML, Gelperin A. DNA-decorated carbon nanotubes for chemical sensing. *Phys Stat Sol b*. 2006;243:3252–3256.
4. Guo Z, Liang L, Liang JJ, Ma YF, Yang XY, Ren DM, Chen YS, Zheng JY. Covalently *b*-cyclodextrin modified single-walled carbon nanotubes: a novel artificial receptor synthesized by 'click' chemistry. *J Nanopart Res*. 2008;10:1077–1083.
5. Ashok Kumar S, Wang SF. Adsorption of ciprofloxacin and its role for stabilizing multi-walled carbon nanotubes and characterization. *Mater Lett*. 2009;63:1830–1833.

6. Tasis D, Tagmatarchis N, Bianco A, Prato M. Chemistry of carbon nanotubes. *Chem Rev*. 2006;106:1105–1136.
7. Munge B, Liu GD, Collins G, Wang J. Multiple enzyme layers on carbon nanotubes for electrochemical detection down to 80 DNA copies. *Anal Chem*. 2005;77:4662–4666.
8. Zhang B, Xing Y, Li Z, Zhou H, Mu Q, Yan B. Functionalized carbon nanotubes specifically bind to α-chymotrypsin's catalytic site and regulate its enzymatic function. *Nano Lett*. 2009;9:2280–2286.
9. Gao Y, Kyratzis I. Covalent immobilization of proteins on carbon nanotubes using the cross-linker 1-ethyl-3-(3-dimethylaminopropyl) carbodiimide—a critical assessment. *Bioconjug Chem*. 2008;19: 1945–1950.
10. Balavoine F, Schultz P, Richard C, Mallouh V, Ebbesen TW, Mioskowski C. Helical crystallization of proteins on carbon nanotubes: a first step towards the development of new biosensors. *Angew Chem Int Ed*. 1999;38:1912–1915.
11. Shim M, Kam NWS, Chen RJ, Li YM, Dai HJ. Functionalization of carbon nanotubes for biocompatibility and biomolecular recognition. *Nano Lett*. 2002;2:285–288.
12. Gomez JM, Romero MD, Fernandez TM. Immobilization of β-glucosidase on carbon nanotubes. *Catal Lett*. 2005;101:275–278.
13. Chen RJ, Bangsaruntip S, Drouvalakis KA, Kam NWS, Shim M, Li YM, Kim W, Utz PJ, Dai HJ. Noncovalent functionalization of carbon nanotubes for highly specific electronic biosensors. *Proc Natl Acad Sci USA*. 2003;100:4984–4989.
14. Karajanagi SS, Vertegel AA, Kane RS, Dordick JS. Structure and function of enzymes adsorbed onto single-walled carbon nanotubes. *Langmuir*. 2004;20:11594–11599.
15. Das D, Das PK. Superior activity of structurally deprived enzyme-carbon nanotube hybrids in cationic reverse micelles. *Langmuir*. 2009;25:4421–4428.
16. Mu Q, Liu W, Xing Y, Zhou H, Li Z, Zhang Y, Ji L, Wang F, Si Z, Zhang B, Yan B. Protein binding by functionalized multiwalled carbon nanotubes is governed by the surface chemistry of both parties and the nanotube diameter. *J Phys Chem C*. 2008;112:3300–3307.
17. Asuri P, Karajanagi SS, Yang H, Yim TJ, Kane RS, Dordick JS. Increasing protein stability through control of the nanoscale environment. *Langmuir*. 2006;22:5833–5836.
18. Matsuura K, Saito T, Okazaki T, Ohshima S, Yumura M, Iijima S. Selectivity of water-soluble proteins in single-walled carbon nanotube dispersions. *Chem Phys Lett*. 2006;429:497–502.
19. Brown JM, Anderson DP, Justice RS, Lafdi K, Belfor M, Strong KL, Schaefer DW. Hierarchical morphology of carbon single-walled nanotubes during sonication in an aliphatic diamine. *Polymer*. 2005;46:10854–10865.
20. Chalikian TV, Macgregor RB Jr. Origins of pressure-induced protein transitions. *J Mol Biol*. 2009;394:834–842.
21. Murayama K, Tomida M. Heat-induced secondary structure and conformation change of bovine serum albumin investigated by Fourier transform infrared spectroscopy. *Biochemistry*. 2004;43:11526–11532.
22. Liu J, Rinzler AG, Dai H, Hafner JH, Bradley RK, Boul PJ, Lu A, Iverson T, Shelimov K, Huffman CB, Rodriguez-Macias F, Shon YS, Lee TR, Colbert DT, Smalley RE. Fullerene pipes. *Science*. 1998;280:1253–1256.
23. Zhong N, Byun HS, Bittrnan R. An improved synthesis of 6-O-monotosyl-6-deoxy-β-cyclodextrin. *Tetrahedron Lett*. 1998;39:2919–2920.
24. Inoue Y, Miyauchi M, Nakajima H, Takashima Y, Yamaguchi H, Harada A. Self-threading of a poly(ethylene glycol) chain in a cyclodextrin-ring: control of the exchange dynamics by chain length. *J Am Chem Soc*. 2006;128:8994–8995.
25. Ingle JDJ, Crouch SR. *Spectrochemical Analysis*. New Jersey: Prentice Hall, 1998.
26. Feng W, Wen H, Xu Z, Wang W. Comparison of perturbed hard-sphere-chain theory with statistical associating fluid theory for square-well fluids. *Ind Eng Chem Res*. 2000;39:2559–2567.
27. Bahr JL, Tour JM. Highly functionalized carbon nanotubes using in situ generated diazonium compounds. *Chem Mater*. 2001;13:3823–3824.
28. Stevens JL, Huang AY, Peng H, Chiang IWJ. Sidewall amino-functionalization of single-walled carbon nanotubes through fluorination and subsequent reactions with terminal diamines. *Nano Lett*. 2003;3:331–336.
29. Li XJ, Chen W, Zhan QW, Dai LM, Sowards L, Pender M, Naik RR. Direct measurements of interactions between polypeptides and carbon nanotubes. *J Phys Chem B*. 2006;110:12621–12625.
30. Aachmann FL, Otzen DE, Larsen KL, Wimmer R. Structural background of cyclodextrin-protein interactions. *Protein Eng*. 2003;16:905–912.
31. Karuppiah N, Sharma A. Cyclodextrins as protein folding aids. *Biochem Biophys Res Commun*. 1995;211:60–66.
32. Machida S, Ogawa S, Shi X, Takaha T, Fujii K, Hayashi K. Cycloamylose as an efficient artificial chaperone for protein refolding. *FEBS Lett*. 2000;486:131–135.
33. Cooper A, Lovatt M, Nutley MA. Energetics of protein-cyclodextrin interactions. *J Incl Phenom Macro*. 1996;25:85–88.
34. Otzen DE, Knudsen BR, Aachmann F, Larsen KL, Wimmer R. Structural basis for cyclodextrins' suppression of human growth hormone aggregation. *Protein Sci*. 2002;11:1779–1787.
35. Griebenow K, Klibanov AM. On protein denaturation in aqueous−organic mixtures but not in pure organic solvents. *J Am Chem Soc*. 1996;118:11695–11700.
36. Yamaguchi KI, Matsumoto T, Kuwata K. Critical region for amyloid fibril formation of mouse prion protein: unusual amyloidogenic properties of the helix 2 peptide. *Biochemistry*. 2008;47:13242–13251.

Manuscript received July 30, 2010, revision received Oct. 22, 2010, and final revision received Jan. 4, 2011.